PHILOSOPHICAL MAGAZINE, 2003, VOL. 83, NO. 6, 711–726

Taylor & Francis
Taylor & Francis Group

Connectivity and percolation in simulated grain-boundary networks

CHRISTOPHER A. SCHUH, ROGER W. MINICH and MUKUL KUMAR†

University of California, Lawrence Livermore National Laboratory, Livermore, California 94550, USA

[*Received 21 June 2002 and accepted in revised form 2 October 2002*]

ABSTRACT

Random percolation theory is a common basis for modelling intergranular phenomena such as cracking, corrosion or diffusion. However, crystallographic constraints in real microstructures dictate that grain boundaries are not assembled at random. In this work a Monte Carlo method is used to construct physically realistic networks composed of high-angle grain boundaries that are susceptible to intergranular attack, as well as twin-variant boundaries that are damage resistant. When crystallographic constraints are enforced, the simulated networks exhibit triple-junction distributions that agree with experiment and reveal the non-random nature of grain-boundary connectivity. The percolation threshold has been determined for several constrained boundary networks and is substantially different from the classical result of percolation theory; compared with a randomly assembled network, about 50–75% more resistant boundaries are required to break up the network of susceptible boundaries. Triple-junction distributions are also shown to capture many details of the correlated percolation problem and to provide a simple means of ranking microstructures.

§1. INTRODUCTION

Intergranular phenomena, including corrosion, cracking and diffusion, have frequently been regarded as percolative phenomena (Wells *et al.* 1989, Lim and Watanabe 1990, Palumbo *et al.* 1991, Aust *et al.* 1994, Watanabe 1994, Pan *et al.* 1995, Gertsman and Tangri 1997, Lehockey *et al.* 1998, Kononenko *et al.* 2001). In this framework, grain boundaries are classified as being either 'susceptible' or 'resistant' to intergranular attack, and random bond percolation theory (for example Stauffer and Aharony (1992)) has commonly been used to predict, firstly, the size scale of susceptible boundary paths or, secondly, the threshold fraction of resistant boundaries required to disrupt the percolating network of susceptible boundaries. For example, Wells *et al.* (1989) have calculated the percolation threshold for randomly assembled two-dimensional (2D) and three-dimensional (3D) grain-boundary networks and applied the results to intergranular stress corrosion cracking data for austenitic stainless steel. Palumbo and co-workers have also predicted the scale of the susceptible grain-boundary network on the basis of random probabilistic analysis and thereby estimated the resistance of microstructures to intergranular attack (Palumbo *et al.* 1991, Aust *et al.* 1994, Lehockey *et al.* 1998).

† Email: mukul@llnl.gov.

Philosophical Magazine ISSN 01478–6435 print/ISSN 1478–6443 online
http://www.tandf.co.uk/journals
DOI: 10.1080/0141861021000056681

For many intergranular phenomena, the class of 'twin-variant' grain boundaries has been correlated with improved physical properties compared with random high-angle grain boundaries, including resistance to self-diffusion, corrosion and cracking (Don and Majumdar 1986, Palumbo and Aust 1992, Watanabe 1993, Thaveeprungsriporn and Was 1996, Palumbo *et al.* 1998, Was *et al.* 1998, Gourges 2002). Within the framework of the coincidence site lattice model (Sutton and Balluffi 1995), they are denoted as $\Sigma = 3^n$ boundaries, where n is a positive integer; among these, only the $\Sigma = 3$, $\Sigma = 9$ and $\Sigma = 27$ twin variants ($n \leqslant 3$) are correlated with improved properties. Because of their desirable properties, these grain boundaries are often promoted through *grain boundary engineering*, which is primarily applied to low or medium stacking fault-energy fcc metals that are susceptible to annealing twinning (Gertsman *et al.* 1994, 1996, Palumbo 1998, Palumbo *et al.* 1998, Randle 1999, Kumar *et al.* 2000). To estimate the resistance of a microstructure to intergranular damage, the fraction f_Σ of resistant boundaries is often measured; clearly, higher values of f_Σ are desirable to reduce the connectivity of susceptible grain boundaries.

As already described above, many workers have used a scalar measure such as f_Σ to predict the connectivity of the grain-boundary network on the basis of random percolation theory and thereby to estimate the resistance of the microstructure to intergranular attack. These efforts are extremely valuable, since f_Σ can now be readily assessed from large metallographic sections using electron back-scatter diffraction (EBSD), and used to predict the performance of materials in service. However, several researchers (for example Gertsman *et al.* (1996), Kumar *et al.* (2000) and Schuh *et al.* (2002a)) have pointed out that boundary connectivity is complicated by the need for crystallographic constraints at triple junctions according to the Σ-product rule (Miyazawa *et al.* 1996):

$$\Sigma a\, \Sigma b = m^2 \Sigma c, \tag{1}$$

where a, b and c denote the three boundaries that meet at the junction, and m is a common divisor of a and b. Equation (1) explicitly dictates that grain-boundary connectivity cannot be regarded as a random binary percolation problem.

In a recent study (Schuh *et al.* 2002a), issues of boundary connectivity were examined experimentally in a Ni-based alloy, by identifying isolated clusters of connected grain boundaries from 2D EBSD data sets. That work demonstrated that the grain-boundary topology developed during sequential grain-boundary engineering processing could not be predicted on the basis of a random assignment of grain boundaries according to f_Σ. Additionally, the coordination of Σ boundaries at triple junctions was found to reflect more accurately the true topology of the grain-boundary network. Preliminary Monte Carlo (MC) simulations of grain-boundary networks have also shown that the non-random character of triple-junction distributions could be accounted for through the application of crystallographic constraints at each junction (Minich *et al.* 2002). In the present article we expand on these issues by exploring connectivity and percolation for simulated 2D grain-boundary networks. We present an MC method for construction of physically reasonable grain boundary networks correlated at triple junctions according to equation (1), and examine the relationships between f_Σ, triple-junction correlations, network connectivity and the percolation threshold for susceptible grain boundaries.

§ 2. Construction of constrained networks

To date, experimental studies of grain-boundary character distribution (GBCD) and grain-boundary networks have been restricted to 2D sections of microstructures. Accordingly, we limit our analysis here to model 2D microstructures based on a regular hexagonal grid. For a binary random bond percolation problem, there are only two types of boundary, for example, 'resistant' and 'susceptible' boundaries. With a random MC approach, the full lattice is then constructed by assigning the hexagonal grid edges as resistant boundaries with a probability f_Σ. As described previously, this random approach does not account for the required constraint imposed by the Σ-product rule (equation (1)) at triple junctions. Unfortunately, equation (1) cannot be simply implemented for the binary classification of 'susceptible' and 'resistant'; numerical values of Σ are required. In principle, the full range of positive odd integers are possible values for Σ in cubic crystals; so, once a boundary is identified as resistant, there is a question as to how it is assigned a Σ value in a physically meaningful manner.

We adopt a simple approach to simulating grain-boundary networks, using four boundary types: three twin variants, $\Sigma = 3$, $\Sigma = 9$ and $\Sigma = 27$, which are all assumed to be 'resistant', and an additional random large-angle boundary type, which is susceptible to intergranular damage and represents all Σ greater than 29. This simplification is quite reasonable for low to medium stacking-fault-energy materials, where the population of low-Σ boundaries is almost entirely twin variants, and more than half comprised $\Sigma = 3$ boundaries. Furthermore, the remaining types of low-Σ boundaries ($\Sigma = 5$, $\Sigma = 7$, $\Sigma = 11$, etc.) not only are infrequently observed in most metals but also are more tenuously linked to special properties (Randle 1999, Gourges 2002). For these reasons, and as a first approximation of the full complexity of grain-boundary networks, we consider only the twin variant boundaries for the purposes of the present simulations.

The construction of a correlated hexagonal grain boundary network proceeds according to the flow chart in figure 1. It is assumed that, of the three boundaries that coordinate a triple junction, two may be assigned on the basis of a random selection procedure; the third boundary is then required to satisfy the constraint imposed by equation (1). Unconstrained boundaries are chosen as follows. Firstly, the boundary is assigned as 'resistant' or 'susceptible' with a probability f_Σ or $1 - f_\Sigma$ respectively; the resistant boundary fraction is specified as an input to the simulation. If the boundary is to be resistant, then it must further be assigned a Σ value of 3, 9 or 27. Here, a second numerical probability is introduced, $A \equiv f_3/f_\Sigma$, which represents the fraction of resistant boundaries that are of type $\Sigma = 3$; A is therefore a measure of twin-boundary prominence. In practice, the value of A is numerically usually between 0.4 and 0.9, based on experiments (Kumar *et al.* 2000, Schuh *et al.* 2002c) and simulations of multiple twinning events (Gertsman and Tangri 1995). Palumbo *et al.* (1992) considered the efficiency of twinning in producing other low-Σ boundaries theoretically and suggested that $A = 2/3$ for the case where each twin boundary coordinates one additional low-Σ boundary. Thus, the value of A is experimentally measurable, is physically meaningful and lies within a relatively narrow range. Although it is beyond the scope of this paper, in principle A may be physically linked to intrinsic material properties such as stacking-fault energy, as well as the processing history of the material.

In the case where a resistant boundary is not $\Sigma = 3$, then it is either $\Sigma = 9$ or $\Sigma = 27$. The boundary is then assigned as a type $\Sigma = 9$ with probability A, and

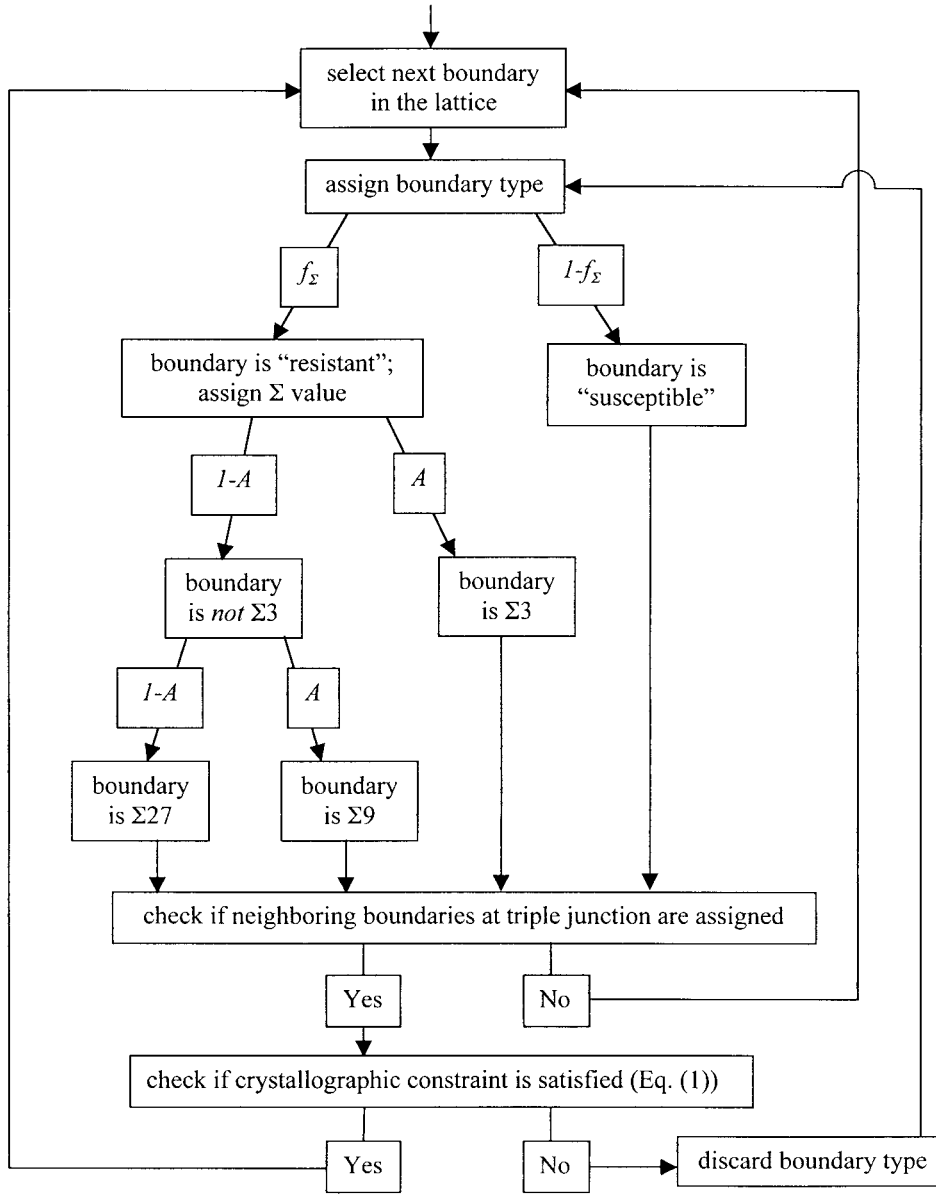

Figure 1. Flow chart illustrating the MC method of assembling grain-boundary networks.

$\Sigma = 27$ with probability $1 - A$. This approach is justified by experimental data (Kumar *et al.* 2000, Schuh *et al.* 2002c), where $f_3/f_\Sigma \approx f_9/(f_9 + f_{27})$, and is physically reasonable as well; two $\Sigma = 3$ boundaries must interact to produce each $\Sigma = 9$ boundary (giving a local value $A = 2/3$), while a $\Sigma = 3$ and $\Sigma = 9$ boundary (or a total of at least three $\Sigma = 3$ boundaries) are required to generate a single $\Sigma = 27$ boundary (giving $A \geqslant 0.5$). Thus, $\Sigma = 3$ boundaries are most prominent among twin variants, and the $\Sigma = 9$ population is larger than that of $\Sigma = 27$ boundaries in roughly the same proportion.

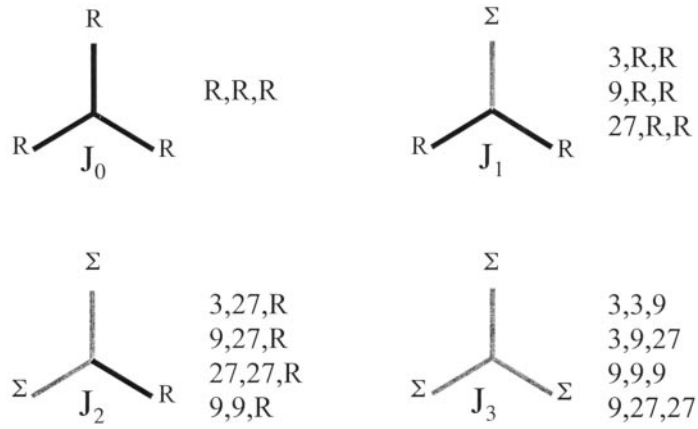

Figure 2. The four types of triple junction, J_i ($i = 0, 1, 2, 3$), shown together with all possible combinations of boundary types that satisfy crystallographic constraints (equation (1)) for the limited population of boundary types used in the MC simulations.

The above approach allows the entire GBCD to be specified using only two parameters, f_Σ and A, and the selection procedure outlined in figure 1 is summarized as follows. The probability f_x of assigning an unconstrained boundary as type x is given as

$$f_3 = f_\Sigma A, \tag{2a}$$

$$f_9 = f_\Sigma (1 - A) A, \tag{2b}$$

$$f_{27} = f_\Sigma (1 - A)^2, \tag{2c}$$

$$f_{\text{Susceptible}} = 1 - f_\Sigma. \tag{2d}$$

As noted earlier, at each triple junction, only two of three boundaries can be regarded as unconstrained, and the third boundary must then be chosen such that it satisfies the constraint of equation (1). All the combinations that meet the constraint for this limited population of boundaries are assembled in figure 2. As shown in the flow chart in figure 1, after each boundary is assigned by the scheme above, the algorithm identifies the adjacent boundaries and checks to see that equation (1) is satisfied. If there is a violation of equation (1), then the boundary is discarded and the assignment process begins again; this process is repeated until an acceptable boundary is selected.

In the present MC scheme, it is important to note that the input or 'local' values of f_Σ and A are not necessarily equal to the 'global' values in the completed network. Because of the nature of the crystallographic constraint, the global values of these parameters evolve during the simulation and, on average, differ from the input values by about 0.1. In the discussions that follow, we always refer to the global values of f_Σ and A ($= f_3/f_\Sigma$) and note that these global quantities parametrize the networks and not the method used to construct them.

§ 3. Triple-junction distributions

A simple metric for boundary connectivity is given by the so-called triple junction distribution, which classifies the node points of the network into four types

(Gertsman and Tangri 1995, Gertsman *et al.* 1996, Randle and Davies 1999, Kumar *et al.* 2000). The type J_i ($i = 0, 1, 2$ or 3) junction coordinates i resistant and $3 - i$ susceptible boundaries, as shown in figure 2. If a triple junction is assembled through a process of random sampling without regard to crystallographic constraint, then the probabilities of forming each junction type are given by

$$J_0 = (1 - f_\Sigma)^3, \tag{3a}$$

$$J_1 = 3f_\Sigma(1 - f_\Sigma)^2, \tag{3b}$$

$$J_2 = 3f_\Sigma^2(1 - f_\Sigma), \tag{3c}$$

$$J_2 = f_\Sigma^3. \tag{3d}$$

In figure 3, this random triple-junction distribution is plotted as a function of f_Σ, for all four types J_i. Also shown in figure 3 are experimental data points from the studies

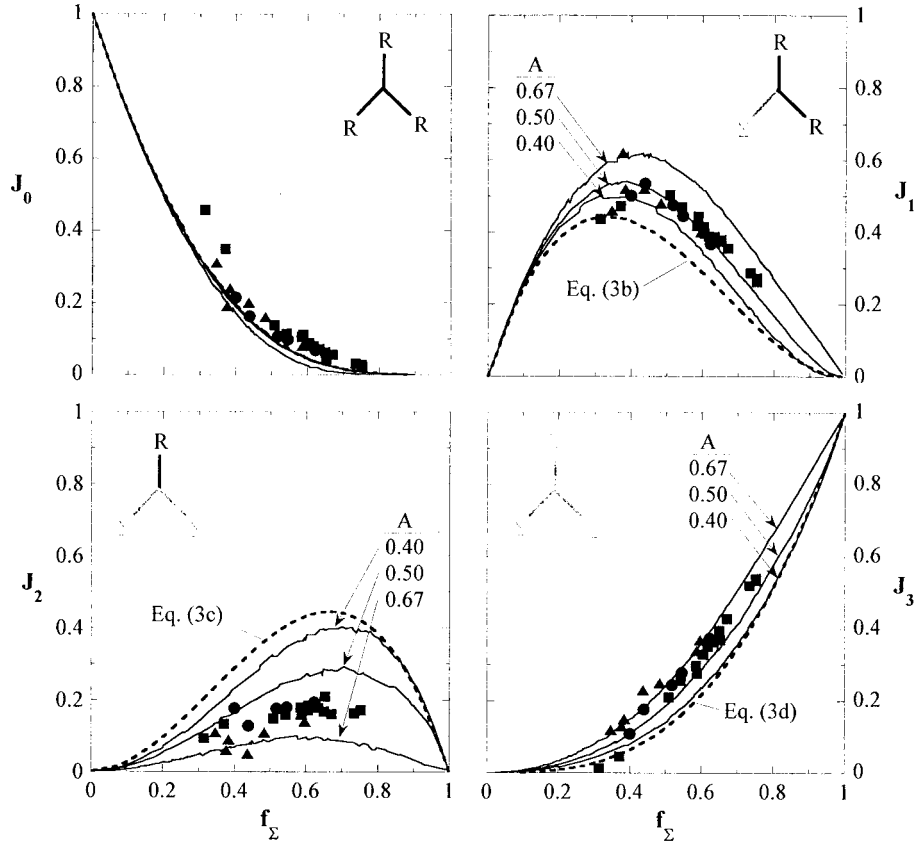

Figure 3. The triple-junction distributions for grain-boundary networks: (- - -) analytical solution based on purely random sampling (equation (3)); (——), constrained lattices constructed using the MC algorithm; (●), experimental data points for Cu and Ni-base alloys from Schuh *et al.* (2002a); (■), experimental data points for Cu and Ni-base alloys from Kumar *et al.* (2000); (▲), experimental data points for Cu and Ni-base alloys from Randle and Davies (1999).

by Randle and Davies (1999), Kumar *et al*. (2000) and Schuh *et al*. (2002a), which show the triple-junction distributions experimentally measured on specimens of Cu and a Ni-based alloy (Inconel 600). For each of these data sets, the number fraction of resistant boundaries has been determined from the following general relation:

$$f_\Sigma = \tfrac{1}{3}(J_1 + 2J_2 + 3J_3). \tag{4}$$

In general, this quantity may be different from the 'special boundary fraction' reported by some workers, calculated on the basis of boundary lengths rather than numbers. As noted by, for example, Randle and Davies (1999) and Kumar *et al*. (2000), the length fraction of resistant boundaries is not expected to correlate with the triple-junction distribution in a straightforward fashion.

As observed elsewhere (Kumar *et al*. 2000, Minich *et al*. 2002), the experimental results assembled in figure 3 cannot be described by equation (3) based on the random assignment of boundaries according to f_Σ. In particular, the frequency of J_2 junctions is substantially below the prediction of equation (3*c*) over the full range of resistant boundary fractions, while the J_1 and J_3 junctions occur more frequently than expected from equation (3). Physically, these results have previously been justified on the basis of crystallographic constraint via equation (1), which suggests that, when two Σ boundaries meet at a triple junction, the third boundary is likely to be of low-Σ type as well. Consequently, J_2 junctions appear only infrequently, and resistant boundaries tend to assemble into J_1 or J_3 junctions instead. The J_0 junctions are not directly affected by crystallographic constraint through equation (1) and thus more closely match the expectations of a random assembly process.

Also shown in figure 3 are the results of MC simulations based on the population of twin-variant boundaries, which incorporate the local crystallographic constraint of equation (1). Here three physically reasonable values of the control parameter A (the twin-boundary prominence) have been used, and an increase in A causes the triple-junction distribution to diverge more strongly from the random case of equation (3). In particular, the constraint causes a substantial depression of the J_2 junction frequency, and somewhat smaller increases in the J_1 and J_3 junctions, in agreement with the experimental data. Furthermore, the MC simulations appear to bracket the experimental data for J_1, J_2 and J_3 from three independent studies on two different materials. Finally, we note that crystallographic constraint has little role in the assembly of J_0 junctions, for which the MC results are very close to both the experimental data and the predictions of equation (3).

For the triple junctions of figure 3, we do not expect that the experimental data should be described by a single value of A, since this parameter will vary with processing history, texture and intrinsic materials properties such as stacking-fault energy. Furthermore, in iterative processing schedules involving multiple twinning events, the value of A has been shown to evolve with f_Σ, in both experiments (Kumar *et al*. 2000, Schuh *et al*. 2002c) and simulations (Gertsman and Tangri 1995). However, it is encouraging that the experimental data, with typical values in the range $A = 0.4$–0.8, are bounded by the simulation results with similar input values.

§ 4. Percolation thresholds

For many material properties that are controlled by intergranular failure mechanisms, the critical design parameter for the grain-boundary network is the percolation threshold for the susceptible boundaries. For example, percolation models have been applied to the analysis of corrosion (Palumbo *et al*. 1991, Aust *et al*.

1994, Lehockey *et al.* 1997), electromigrative diffusion (Kononenko *et al.* 2001) and cracking (Lim and Watanabe 1990, Palumbo *et al.* 1991, Aust *et al.* 1994, Watanabe 1994, Pan *et al.* 1995, Gertsman and Tangri 1997), where it is detrimental to have a percolating network of susceptible boundaries. However, all these analyses have incorporated the basic assumption of random percolation theory, namely that boundary types (susceptible versus resistant) can be selected at random from a known distribution. With this assumption, the classical results from percolation theory apply; the percolation threshold on a 2D hexagonal lattice is $f_\Sigma^c = 0.347$ (Stauffer and Aharony 1992). Below this value there is an infinite percolating cluster of susceptible boundaries, which breaks up above the threshold. To our knowledge, there is no existing theory that gives the percolation threshold for a lattice that obeys a local constraint equation such as equation (1) at each node; we address this issue in the following.

Percolation was studied on hexagonal grids with 100 grains on each side, involving about 3×10^4 grain boundaries. For given input values of f_Σ and A, several hundred lattices were constructed, and the fraction of networks containing a percolative susceptible grain boundary cluster was calculated. Figure 4 shows this value Π as a function of the resistant boundary fraction f_Σ. The black line in figure 4 is the result of such simulations for the case where susceptible and resistant boundaries are assigned by a random selection process, and no constraint is enforced. As expected, there is a critical value of f_Σ that separates regimes of percolating or non-percolating susceptible grain-boundary networks. In figure 4 this transition is not abrupt at the theoretical value of $f_\Sigma^c = 0.347$ (Stauffer and Aharony 1992) but exhibits some spread around this value; this is a finite-size effect that would disappear if the simulated lattice size were increased towards infinity.

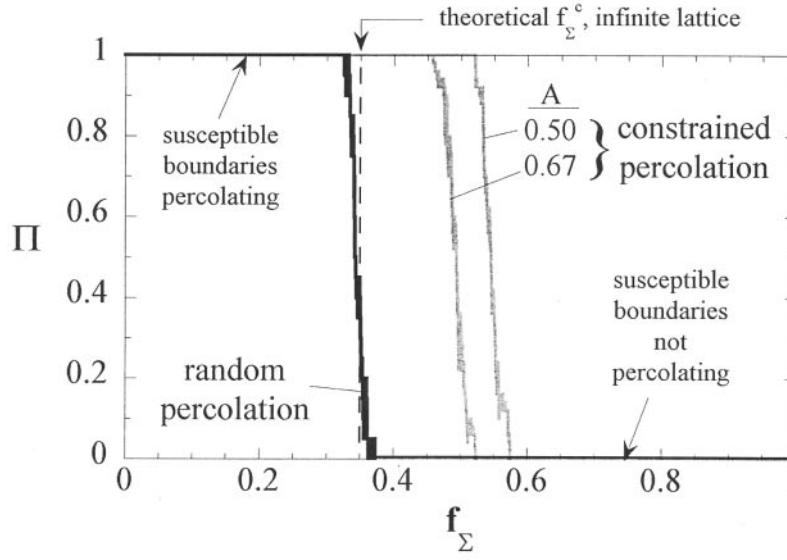

Figure 4. The probability Π that susceptible boundaries percolate on a finite grid measuring 100 grains on a side, as a function of the resistant boundary fraction f_Σ. The black line illustrates the results for unconstrained assignment of boundaries, which agrees with the results of classical random percolation theory. The grey lines show the shift of the percolation threshold when crystallographic constraints are enforced.

The grey lines in figure 4 illustrate the effect of crystallographic constraint on the percolation threshold, for two example values of the twin prominence A. Local constraints are found to impact substantially on the percolation behaviour, giving percolation thresholds of $f_\Sigma^c \approx 0.5$ and $f_\Sigma^c \approx 0.55$ for input values $A = 0.67$ and $A = 0.5$ respectively. Figure 5 summarizes the results of our MC simulations for four different reasonable values of A, comparing the resulting percolation thresholds with that expected on the basis of a random assembly process. Over the range $A = 0.4$–0.75, the percolation threshold is substantially higher than the value of $f_\Sigma^c = 0.347$ for the random assembly case. Furthermore, the changes in f_Σ^c with A are non-monotonic; there appears to be an inflection near $A = 0.67$, beyond which the percolation threshold rises. This increase may be expected, since in the limit where $A \to 1$, all the resistant boundaries are type $\Sigma = 3$. According to the constraint expressed in figure 2 and equation (1), it then becomes impossible for a triple junction to coordinate either two or three resistant boundaries; only the 3,R,R and R,R,R combinations in figure 2 would be allowed. Accordingly, it would become impossible to break up the percolating susceptible boundary network, and the percolation threshold should diverge to unity. Of course, in this limit, the resistant fraction cannot exceed $f_\Sigma = 1/3$; so the susceptible boundary network cannot be significantly disrupted. The upward concavity of the data in figure 5 is thus reasonable and confirms that crystallographic constraint necessarily increases the percolation threshold; there is apparently no special case where a constrained lattice can approach the threshold of a randomly assembled lattice.

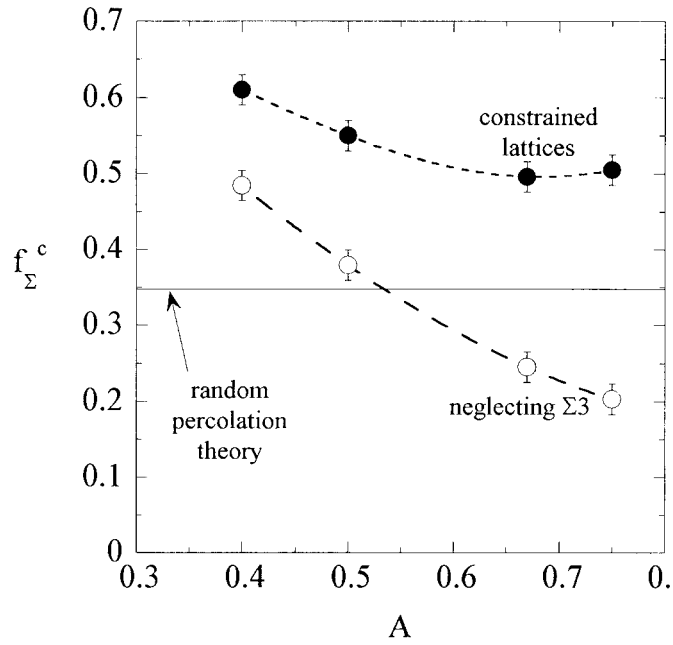

Figure 5. Percolation thresholds for susceptible boundaries, in crystallographically constrained 2D lattices (●), plotted as a function of the twin-boundary prominence A. Also shown are the percolation thresholds that result when $\Sigma = 3$ boundaries are excluded from the analysis (○).

From the viewpoint of materials design, the results presented in figures 4 and 5 are of prime importance. If engineering materials are to be qualified as 'resistant' to some form of intergranular attack, then f_Σ must exceed the percolation threshold of the susceptible boundary network. The substantially higher percolation threshold for crystallographically constrained lattices (figures 4 and 5) indicates that the grain-boundary network must be judged according to a higher standard than random percolation theory would suggest. Also, figure 5 reveals that the exact value of the percolation threshold may be a function of details in the GBCD. For example, the multiple-twinning simulations of Gertsman and Tangri (1995) indicate that the value of A decreases with increasing f_Σ; experimental data (Kumar *et al.* 2000, Schuh *et al.* 2002c) show a similar trend. The percolation threshold then becomes a 'moving target' that increases slightly with increasing f_Σ according to figure 5. Traditionally, the goal of grain-boundary engineering has been solely to increase the value of f_Σ; the present results suggest that a high prominence of $\Sigma = 3$ twin boundaries ($0.6 < A < 0.8$) may also be desirable to reduce the percolation threshold.

Although the present results are limited to 2D lattices, the relationship between percolation and cluster properties in two and three dimensions is well known for standard percolation problems (Stauffer and Aharony 1992), and there are scaling laws that link these problems with those in even higher-dimensional spaces as well. At present, the appropriate scaling laws for the present constrained percolation problem are not yet known; future research in this area will focus on scaling and extension to higher dimensions. One limitation to the power of such scaling laws is the necessity that the microstructure (i.e. the GBCD) be isotropic. Fortunately, experimental work has repeatedly shown that twin-dominated microstructures tend to be texture-free and essentially isotropic. At any rate, the present observation of a shift in the percolation thresholds in two dimensions strongly suggest that crystallographic constraint should also increase the percolation thresholds in three dimensions.

In the literature on grain-boundary engineering, it has been observed that $\Sigma = 3$ twin boundaries (especially coherent twin boundaries) may not strongly affect the connectivity of the grain-boundary network, since these boundaries do not replace susceptible boundaries *per se* but rather develop in the interior of existing grains (Alexandreanu *et al.* 2001, Alexandreanu and Was 2001). We believe that this line of reasoning partly explains why the percolation thresholds in constrained lattices are higher than those of a randomly assembled lattice. In some sense, the $\Sigma = 3$ boundaries may contribute less than other Σ boundaries to the topology of the network; so their inclusion in the analysis inflates f_Σ without a commensurate reduction of the susceptible boundary connectivity. If this point of view were strictly interpreted, then twin boundaries would be completely excluded from the analysis, counting neither as resistant nor as susceptible. This philosophy has been followed in some experimental studies where coherent $\Sigma = 3$ boundaries were neglected (Crawford and Was 1992, Thaveeprungsriporn and Was 1996, 1997, Alexandreanu *et al.* 2001), while other studies have emphasized the importance of $\Sigma = 3$ boundaries in the grain-boundary network (Kumar *et al.* 2000).

Excluding all $\Sigma = 3$ boundaries from the analysis amounts to a redefinition of the resistant boundary fraction according to:

$$f'_\Sigma = f_\Sigma \frac{1 - A}{1 - f_\Sigma A}, \tag{5}$$

where the quantities on the right-hand side are those already defined (which include the $\Sigma = 3$ boundaries), and the new quantity, f'_Σ, is the resistant fraction of boundaries when the $\Sigma = 3$ boundaries are ignored. In figure 5, the open circles show the percolation thresholds for constrained lattices, after correcting the data with equation (5). Of course, the exclusion of $\Sigma = 3$ boundaries does reduce the percolation threshold, bringing it closer to that expected for a randomly assembled lattice. However, if the $\Sigma = 3$ boundaries played no role whatever in determining the connectivity of the boundary network, then the corrected data in figure 5 should collapse on to a horizontal line. Such is clearly not the case. In a statistical sense, then, the $\Sigma = 3$ boundaries do appear to impact the connectivity of the network; simply neglecting these boundaries does not reduce the problem to one of a random-assembly process. Therefore, these simulations offer no reason why the $\Sigma = 3$ boundaries should be neglected from the GBCD analysis. Of course, the present MC networks are only simple representations of true microstructures and do not capture the physics of twinning. Most notably, there is no differentiation between coherent and incoherent $\Sigma = 3$ boundaries in the present simulations; more detailed physical simulations may yield somewhat different conclusions in the role of $\Sigma = 3$ boundaries. Also, since equation (1) is strictly valid only for exact coincident-site lattice (CSL) orientations, the present simulations have not allowed for small deviations from ideal twin or twin-variant orientations.

§ 5. Microstructural rankings

A topic of perennial interest to the field of grain-boundary engineering is ranking of microstructures on the basis of susceptibility to intergranular attack. Traditionally, the resistant boundary fraction f_Σ has been used for this purpose (Palumbo *et al.* 1991, 1998, Aust *et al.* 1994, Lehockey *et al.* 1998). However, because grain-boundary networks do not conform to standard percolation theory, f_Σ is not expected to correlate with the size scale of susceptible boundary clusters. Recent experimental work has led to the development of a new ranking criterion in comparable dimensionless units with the resistant boundary fraction, based on the triple-junction types:

$$\left(\frac{J_2}{1 - J_3}\right)^{1/2}. \tag{6}$$

This ranking criterion was advanced by Kumar *et al.* (2000) on the basis of a crack arrest argument.

In recent experimental work by Schuh *et al.* (2002a), five different specimens of Inconel 600 were analysed to assess the scale of the largest path of susceptible boundaries in the microstructure. Those workers found that the criterion of equation (6) provided a true quantitative ranking of the microstructures, while f_Σ was more prone to ranking errors and was not as quantitatively accurate. That study, while suggestive, was based on only five data points and was prone to several sources of experimental error. The present MC technique allows many networks to be readily constructed and analysed, without substantial limitations on the size or quality of the data. We have therefore performed detailed analytical work to classify the size and shape of grain-boundary clusters, using the same techniques proposed by Schuh *et al.* (2002a). Qualitatively, we find identical results with that experimental work. Specifically, the ranking criterion of Kumar *et al.* (2000) (equation (6)) is consistently

a more accurate predictor of the size scale of susceptible boundary clusters than is the resistant boundary fraction. Although this has been found to be true for many thousands of simulated networks, we present here just one example that particularly highlights this important result.

Figure 6 shows the relationship between the two ranking parameters and the size of the susceptible boundary network for 56 simulated lattices. All these lattices exhibited a resistant boundary fraction within a very narrow range: $f_\Sigma = 0.70 \pm 0.01$. The internal control parameter was also constrained to a narrow range of physically reasonable values: $A = 0.62 \pm 0.11$. The quantity plotted in figure 6, D_{90}, represents the maximum linear dimension (caliper dimension) of a cluster of susceptible boundaries, in units of grain edge length; the subscript 90 here refers to the ninetieth percentile of all boundary clusters in the microstructure. In essence, 90% of all susceptible boundary paths are smaller than D_{90}, which is a scalar measure of the susceptible boundary connectivity.

Figure 6 (*a*) shows the relationship between f_Σ and the susceptible boundary path lengths. Since all the data were acquired on lattices with similar values of f_Σ, this figure simply shows the amount of scatter in D_{90} for a given resistant boundary fraction. If f_Σ were the only microstructural descriptor available, then the scale of susceptible boundary paths could only be approximated to within about ± 25 grain edge lengths. If some of the higher values of D_{90} are treated simply as outliers, there is still an uncertainty of ± 10 or more grain edges. In short, f_Σ cannot accurately predict the size scale of potential failure paths.

Figure 6 (*b*) shows the same data points, now plotted against the ranking criterion of equation (6) based on the triple-junction distributions of the simulated lattices. Compared with the vertical trend in figure 6 (*a*), the data in figure 6 (*b*) have spread on to a well-defined curve, where D_{90} is a sensitive function of the ranking criterion.

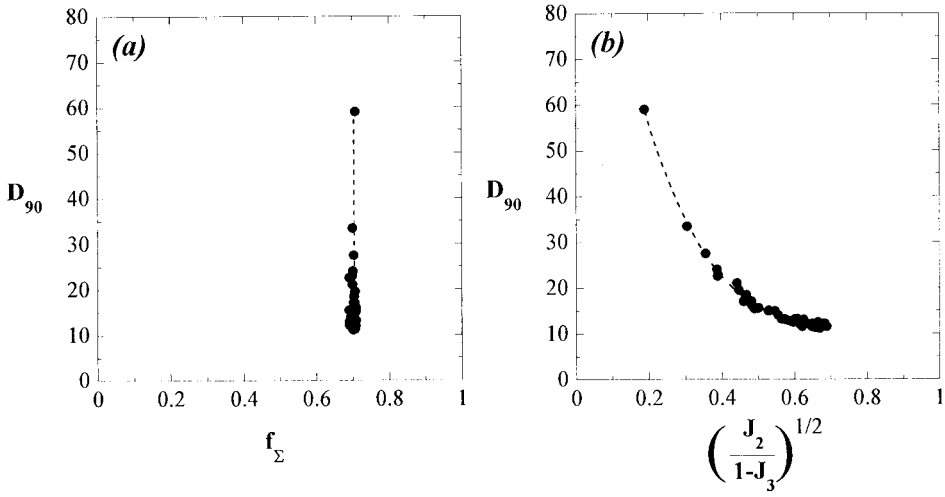

Figure 6. Examples of material ranking based on (*a*) f_Σ or (*b*) the criterion of equation (6). The parameter D_{90} is the size of the ninetieth percentile cluster of susceptible grain boundaries in units of the grain edge length; 90% of susceptible boundary paths are smaller than D_{90}. Whereas D_{90} is poorly predicted by f_Σ in (*a*), it is sensitively dependent on the criterion of equation (6) in (*b*). For these simulations, $A = 0.62 \pm 0.11$.

Thus, if the triple-junction distribution of the microstructure can be assessed, then the scale of susceptible boundary clusters can be uniquely determined with little error. From a physical point of view, equation (6) incorporates subtle issues of boundary connectivity that are not captured by f_Σ. These connectivity variations arise owing to changes in the details of the GBCD, since many GBCDs are possible for a single value of f_Σ. Although we have parametrized all the subtle variations in GBCD into the scalar value of A in the present simulations, the concepts revealed here are general; the connectivity of the grain-boundary network is in part dictated by the GBCD, independently of f_Σ. Consequently, from a materials ranking point of view, we find that equation (6) (figure 6(*b*)) is much more useful and reliable than f_Σ (figure 6(*a*)), which can never fully characterize the microstructure.

It is important to note that experimentally the values of J_2 and J_3 are usually derived on the basis of the full set of CSL boundaries (up to $\Sigma = 29$), whereas the present MC model neglects the majority of these boundaries and focuses only on the twin variants. This difference raises the question as to how important the non-$\Sigma = 3^n$ boundaries are in terms of the connectivity of the random boundary network; if twin-variant boundaries only rarely assemble into J_2 junctions, then it is possible that non-$\Sigma = 3^n$ boundaries are largely responsible for those junctions in experimental microstructures. Although the 'susceptible' or 'resistant' nature of such boundaries may be open to question, we find that experimental triple-junction distributions such as those in figure 3 are qualitatively very similar whether or not the non-$\Sigma = 3^n$S boundaries are included in the analysis (Schuh *et al.* 2002b). Furthermore, preliminary MC simulations using the full range of positive odd integers for Σ exhibit the same qualitative features as the present twin-variant-based model (Stölken *et al.* 2001). Thus, although the present model is quite simple, we believe that it captures the essential statistical features of the grain boundary network.

The criterion of equation (6) contains information about the nearest-neighbour correlations between grain boundaries and has been found here and elsewhere to correlate well with the connectivity of the boundary network. These findings suggest that only nearest-neighbour information is necessary to capture the network topology fully and that no higher-order correlations are required. To test this hypothesis, we have conducted a series of simulations in which grain boundary types were assigned (according to figure 1) around isolated triple junctions, which were not assembled into a connected lattice. We find that, to within a very narrow margin of error, the triple-junction distributions are identical with those found when a 2D lattice is constructed. This result is illustrated for the J_2 and J_3 junctions in figure 7.

Since crystallographic constraints are only applied locally at each triple junction, it is intuitively reasonable that long-range correlations play a minor role in grain-boundary networks. Any long-range structure that arises in the network can therefore be reasonably regarded simply as emergent structure arising from cluster growth processes, as in percolation theory. These results also imply that the triple-junction distribution is unaffected by other topological features of the grain-boundary network, such as variation in the number of grain edges around each grain. Finally, the results in figure 7 also lend credence to the use of equation (6) to rank microstructures, since the triple-junction distribution used in equation (6) captures the dominant correlations in the network.

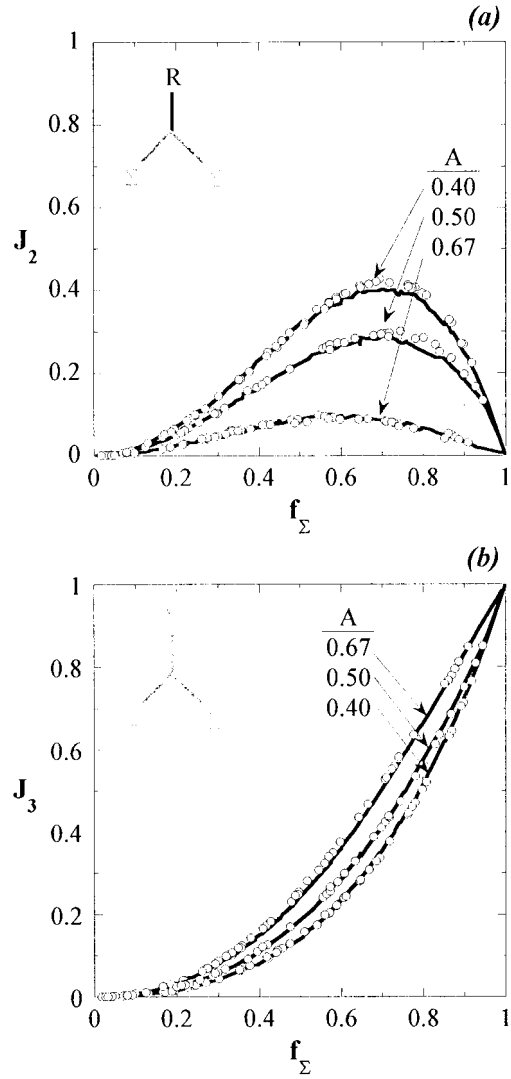

Figure 7. Distributions of (*a*) J_2 and (*b*) J_3 triple junctions determined from MC simulations on a hexagonal lattice (——), and on isolated triple junctions that are not connected to one another (○).

§ 6. Summary and conclusions

Connectivity and percolation of susceptible grain boundaries are of considerable interest to intergranular degradation processes such as corrosion and cracking. Although many previous researchers have treated these phenomena using a random bond percolation approach, grain boundaries cannot be assembled in a random fashion because of crystallographic constraints at triple junctions. Here we have developed an MC approach to the simulation of grain-boundary networks, based on the assumption that twin-variant boundaries are resistant to intergranular attack. The method has been used to study connectivity and percolation of 2D grain-boundary networks, with the following major results.

(1) Using a single, narrowly confined control parameter, the MC method can accurately describe triple-junction distributions recently measured on several different metals. These distributions are significantly different from predictions of random percolation theory, because of the tendency for damage-resistant boundaries to aggregate in the microstructure.
(2) Crystallographic constraints on the grain-boundary network substantially change the percolation threshold for susceptible grain boundaries. Random percolation theory predicts a break-up of the susceptible boundary network when the resistant boundary fraction exceeds $f_\Sigma^c = 0.347$; the constrained lattices exhibit a percolation threshold above $f_\Sigma^c = 0.50$.
(3) Whereas the resistant boundary fraction has commonly been used to rank microstructures for their susceptibility to intergranular failure, the MC simulations show that this parameter is not sensitive to the complex topologies found in grain-boundary networks. For a single value of f_Σ, many GBCDs are possible, and large variations in the length of susceptible boundary paths are found. In contrast, a ranking based on triple-junction distributions is more quantitatively accurate, since these distributions capture the dominant correlations in the network.

Acknowledgements

This work was performed under the auspices of the US Department of Energy at the University of California Lawrence Livermore National Laboratory under contract W-7405-Eng-48.

References

Alexandreanu, B., Capell, B., and Was, G. S., 2001, *Mater. Sci. Engng*, **A300**, 94.
Alexandreanu, B., and Was, G. S., 2001, *Phil. Mag.* A, **81**, 1951.
Aust, K. T., Erb, U., and Palumbo, G., 1994, *Mater. Sci. Engng*, **A176**, 329.
Crawford, D. C., and Was, G. S., 1992, *Metall. Trans.* A, **23**, 1195.
Don, J., and Majumdar, S., 1986, *Acta metall.*, **34**, 961.
Gertsman, V. Y., Janecek, M., and Tangri, K., 1996, *Acta mater.*, **44**, 2869.
Gertsman, V. Y., and Tangri, K., 1995, *Acta metall. mater.*, **43**, 2317; 1997, *Acta mater.*, **45**, 4107.
Gertsman, V. Y., Tangri, K., and Valiev, R. Z., 1994, *Acta metall. mater.*, **42**, 1785.
Gourges, A.-F., 2002, *Mater. Sci. Technol.*, **18**, 119.
Kononenko, O. V., Matveev, V. N., and Field, D. P., 2001, *J. Mater. Res.*, **16**, 2124.
Kumar, M., King, W. E., and Schwartz, A. J., 2000, *Acta mater.*, **48**, 2081.
Lehockey, E. M., Palumbo, G., Brennenstuhl, A., and Lin, P., 1997, *Mater. Res. Soc. Symp. Proc.*, **458**, 243.
Lehockey, E. M., Palumbo, G., Lin, P., and Brennenstuhl, A., 1998, *Metall. Mater. Trans.*, A, **29**, 387.
Lim, L. C., and Watanabe, T., 1990, *Acta metall. mater.*, **38**, 2507.
Minich, R. W., Schuh, C. A., and Kumar, M., 2002, *Phys. Rev.* B, **66**, 052 101.
Miyazawa, K., Iwasaki, Y., Ito, K., and Ishida, Y., 1996, *Acta crystallogr.* A, **52**, 787.
Palumbo, G., 1998, Metal Alloys Having Improved Resistance to Intergranular Stress Corrosion Cracking, US Patent no. 5, 81F, 193.
Palumbo, G., and Aust, K. T., 1992, *Materials Interfaces*, edited by D. Wolf and S. Yip (London: Chapman & Hall), p. 190.
Palumbo, G., Aust, K. T., Erb, U., King, P. J., Brennenstuhl, A. M., and Lichtenberger, P. C., 1992, *Phys. Stat. sol.*, **131**, 425.
Palumbo, G., King, P. J., Aust, K. T., Erb, U., and Lichtenberger, P. C., 1991, *Scripta metall. mater.*, **25**, 1775.
Palumbo, G., Lehockey, E. M., and Lin, P., 1998, *J. Metals*, **50**, 40.

Pan, Y., Olson, T., and Adams, B. L., 1995, *Can. Metall. Q.*, **34**, 147.
Randle, V., 1999, *Acta mater.*, **47**, 4187.
Randle, V., and Davies, P., 1999, *Proceedings of the Fourth International Conference on Recrystallization and Related Phenomena*, edited by T. Sakai and H. G. Suzuki (Sendai: Japan Institute of Metals), p. 501.
Schuh, C. A., Kumar, M., and King, W. E., 2002a, *Acta Mater.* (in press); 2002b, *Z. Metallk.* (in press); 2002c, *Interface Sci.* (submitted).
Stauffer, D., and Aharony, A., 1992, *Introduction to Percolation Theory* (London: Taylor & Francis).
Stölken, J. S., Minich, R. W., Kumar, M., and Schuh, C. A., 2001, *Symposium on Statistical Mechanical Modeling in Materials Research, Materials Research Society Fall Meeting*, Boston, Massachusetts, 2001.
Sutton, A. P., and Balluffi, R. W., 1995, *Interfaces in Crystalline Materials* (Oxford Science Publications).
Thaveeprungsriporn, V., and Was, G. S., 1996, *Scripta mater.*, **35**, 1; 1997, *Metall. Mater. Trans.* A, **28**, 2101.
Was, G. S., Thaveeprungsriporn, V., and Crawford, D. C., 1998, *J. Metals*, **50**, 44.
Watanabe, T., 1993, *Mater. Sci. Engng*, **A166**, 11; 1994, *ibid.*, **A176**, 39.
Wells, D. B., Stewart, J., Herbert, A. W., Scott, P. M., and Williams, D. E., 1989, *Corrosion*, **45**, 649.